Plant Physiology and Biochemistry 142 (2019) 143–150

Contents lists available at ScienceDirect

Plant Physiology and Biochemistry

journal homepage: www.elsevier.com/locate/plaphy

Research article

Differential fluoride uptake induces variable physiological damage in a non-aromatic and an aromatic indica rice cultivar

Aditya Banerjee, Aryadeep Roychoudhury*, Puja Ghosh

Post Graduate Department of Biotechnology, St. Xavier's College (Autonomous), 30, Mother Teresa Sarani, Kolkata, 700016, West Bengal, India

ARTICLE INFO

Keywords:
Fluoride
Rice
Damage
Metabolic pathways
Uptake

ABSTRACT

The current study illustrates the systemic damages caused by increasing concentration of fluoride in non-aromatic rice variety, IR-64 and aromatic rice Gobindobhog (GB). Analysis of the physiological parameters like shoot length, root length and electrolyte leakage along with crucial damage indices like chlorophyll, malondialdehyde, H_2O_2 and protease activity indicated higher fluoride adaptation in GB compared to IR-64. IR-64 exhibited unregulated fluoride bioaccumulation when exposed to 25 mg L^{-1} NaF stress, whereas fluoride uptake in GB was much regulated. Gene expression studies proposed that *CLC2* rather than *CLC1* mediated the fluoride import. Fluoride also triggered higher P-H^+/ATPase accumulation in GB compared to IR-64, thus highlighting efficient homeostasis in stressed GB. Unlike IR-64, GB could maintain photosynthesis (*RuBisCo* expression), sugar metabolism (*α-amylase* expression and activity), glycolysis and Krebs cycle even under high concentration of fluoride stress. Fluoride also inhibited nitrate reductase activity in both the cultivars. The present research illustrates differential phytotoxicity emerging out of fluoride accumulation in rice seedlings, highlighting that IR-64 is a highly susceptible variety, whereas GB exhibits physiological plasticity and is better adapted to higher concentrations of fluoride.

1. Introduction

Fluorine ranks 13th in the list of the most abundant elements found in nature, with about 950 mg L^{-1} stored as fluorides within the earth's crust. Fluoride (F^-) acts as a toxic xenobiotic in the ecological food chain (Banerjee and Roychoudhury, 2019a). The World Health Organization (WHO) has strictly debarred ingestion of F^- beyond the safe limit of 1.5 mg L^{-1}. Doses of F^- above this limit can result in severe fluorosis along with neurological disorders in animals and humans (Choubisa, 2013). The extent of F^- contamination in India has been recorded to be as high as 48 mg L^{-1} (Susheela, 1999). Such contamination has been shown to hinder absorption and transport of water and minerals, which are the prerequisites for normal physiological and biochemical processes of plants. F^- is an accumulative poison and is absorbed by the plants via the chloride channels in roots and translocated to the transpiratory tissues by xylematic flow (Banerjee and Roychoudhury, 2019b). It was found that the vacuolar voltage gated chloride channels (*CLC1* and *CLC2*) were induced on exposure to NaCl (Nakamura et al., 2006). F^- ions having a smaller diameter compared to chloride ions might enter the root tissues via these reported chloride channels. Reduced plasma membrane H^+/ATPase (P-H^+/ATPase) activity was observed in semi-arid plant species grown under F^- stress (Baunthiyal and Sharma, 2014).

Excessive availability of F^- within the plant tissues has been shown to incite various toxicity symptoms like inhibition in germination potential, growth and productivity, biomass, photosynthesis and nitrogen assimilation, chlorosis or chlorophyll (Chl) breakdown, reduced ribulose-1,5-bispohosphate carboxylase/oxygenase (RuBisCo) activity, alterations in the activity of enzymes and protein synthesis, culminating ultimately in oxidative stress conditions (Banerjee and Roychoudhury, 2019a). Uncontrolled production of reactive oxygen species (ROS) like hydrogen peroxide (H_2O_2), superoxide, hydroxyl radicals, etc. trigger membrane peroxidation along with the release of cytotoxic products including malondialdehdye (MDA) in the affected tissues (Debska et al., 2012). Stress conditions lead to protein inactivity and proteolytic breakdown by the increased activity of protease during abiotic stress (Debska et al., 2012). The enzymes like pyruvate dehydrogenase (PyrDH), malate dehydrogenase (MDH) and succinate dehydrogenase (SDH), belonging to the Krebs cycle, are strongly inhibited under abiotic stress conditions in the susceptible varieties (Che-Othman et al., 2017). The rate limiting enzyme of nitrogen acquisition, viz., nitrate reductase (NR) was found to be inhibited in mulberry seedlings during fluoride stress (Rao et al., 2013).

Bioaccumulation of F^- in the vegetative tissues and grains of edible

* Corresponding author.
E-mail address: aryadeep.rc@gmail.com (A. Roychoudhury).

https://doi.org/10.1016/j.plaphy.2019.06.034
Received 22 April 2019; Received in revised form 25 June 2019; Accepted 26 June 2019
Available online 28 June 2019
0981-9428/

cereals is a direct threat to the entire food chain (Mondal and Gupta, 2015). It has been suggested that high bioaccumulation of F^- within the vegetative tissues stands out as an indicator of high fluoride accumulation within the edible grains (Gupta et al., 2009). Rice is a water-intensive food crop of South East Asian countries, cultivated widely in Bangladesh and in several Indian states facing acute endemic fluorosis due to high F^- content in groundwater (Meenakshi, 2006). Previous reports presented very preliminary insights into the physiological injuries caused by F^- accumulation in indica rice varieties. The importance of the present work from the agricultural perspective as well as environmental point of view was with respect to the identification of high-F^- accumulating rice variety, so as to avoid cultivation of such variety in land stretches irrigated with F^--infested groundwater that might deteriorate production as well as seed quality. It is also imperative to decipher the nature of damages and detrimental effects on rice during F^- stress. Therefore, the aim of our study in the present manuscript was to assess the response of two varieties of indica rice, viz., IR-64 and Gobindobhog (GB) to long-term F^- stress for 20 days, using two different F^- concentration, viz., 15 mg L^{-1} and 25 mg L^{-1}. IR-64 was developed by International Rice Research Institute (IRRI), Philippines, as a high-quality and high-yielding mega variety. The popularity of IR-64 cultivation lies due to its early maturation and disease resistance traits along with excellent cooking quality, intermediate amylose content, gelatinization temperature and commendable taste (Mackill and Khush, 2018). This variety has been cultivated across 10 million hectares of land globally and has been used for thousands of crosses and development of new cultivars (Mackill and Khush, 2018). GB, on the contrary, is an endogenous aromatic rice cultivar of West Bengal (the rice bowl of India) largely known for its superior fragrance, palatability and use in preparation of delicacies. This cultivar is widely produced in such districts like Hooghly, Howrah, Nadia, 24 Parganas and Burdwan of West Bengal (Roychoudhury et al., 2008).

The varietal differences in biochemical and molecular mechanism to F^- tolerance were studied by comparing basic physiological parameters like percentage of germination, root and shoot length, and electrolyte leakage. The F^- content in the roots and shoots of the stressed cultivars was measured. The expression of *CLC1* and *CLC2* was analyzed to understand the mechanism of F^- uptake. The expression and accumulation of P-H^+/ATPase, involved in maintaining ionic homeostasis was studied. The parameters associated with damages like Chl degeneration, *RuBisCo* expression, accumulation of MDA, H_2O_2 and protease activity were measured. The effect of increasing F^- concentration on the glycolytic pathway was analyzed by studying the expression of genes like *phosphofructokinase*, *fructose-1,6-bisphosphatase* (*FBPase*) and *phosphoglucomutase* (*PGmutase*). The activity of PyrDH, SDH and MDH was documented to understand the effects of F^- stress on Krebs cycle. The expression and activity of α-amylase represented the effect of F^- on sugar metabolism, whereas the effect of F^- on nitrogen assimilation was deciphered by studying the activity of NR. Thus, the present study revealed the physiological, biochemical and molecular basis of F^--induced damages at the varietal level in rice.

2. Materials and methods

2.1. Plant materials, growth conditions and stress treatment

The seeds of *Oryza sativa* L. cv. IR-64 were procured from Chinsurah Rice Research Station (Hooghly, West Bengal, India) and those of the aromatic cv. Gobindobhog (GB) were obtained from Bidhan Chandra Krishi Viswavidyalaya (Nadia, West Bengal, India). The seeds were surface sterilized with 0.1% (w/v) $HgCl_2$ for 20 min, washed extensively, and placed over sterile gauge in Petridishes (three sets for each variety) supplemented with either 15 mg L^{-1} [15 parts per million (ppm)] or 25 mg L^{-1} (25 ppm) sodium fluoride (NaF) for imposing stress. The plates containing double distilled water were used as control sets. The solution was changed every two days. Thus, six sets of samples were maintained:

Set 1: IR-64 seeds imbibed in double distilled water only.
Set 2: IR-64 seeds imbibed in 15 mg L^{-1} NaF.
Set 3: IR-64 seeds imbibed in 25 mg L^{-1} NaF.
Set 4: GB seeds imbibed in double distilled water only.
Set 5: GB seeds imbibed in 15 mg L^{-1} NaF.
Set 6: GB seeds imbibed in 25 mg L^{-1} NaF.

The seedlings of both the varieties were maintained and grown as above for a total period of 20 days at 32 °C under 16 h light and 8 h dark photoperiodic cycle with 50% relative humidity and 700 μmol photons m^{-2} s^{-1} in a plant growth chamber (N.R. Scientific, India) as previously standardized (Roychoudhury et al., 2008). The NaF concentration and stress exposure was standardized by performing preliminary experiments and following Gupta et al. (2009) who had exposed *Oryza sativa* cv. Satabdi with 10, 20 and 30 mg L^{-1} NaF for 15 days. The varietal differences were increasingly visible during prolonged exposure to NaF concentrations for 20 days (data not shown).

2.2. Analysis of physiological changes brought about by F^- stress

2.2.1. Estimation of percentage of germination and measurement of root and shoot length

The percentage of germination was calculated for a total of 200 seeds in each set of control and treated varieties. The length of the shoot and primary root were measured from 100 seedlings of each category and for each grown condition in three independent experiments.

2.2.2. Estimation of the percentage of electrolyte leakage (EL)

For measuring EL, 0.1 g of freshly harvested leaf samples were rinsed thrice with de-ionized water and subsequently incubated in 10 ml of deionized water. The initial conductivity in the solution was measured after 22 h at room temperature (25 °C) using the conductivity meter (Digital Instruments Corporation, D-511). Total conductivity was obtained after boiling the samples for 30 min. The results were expressed as percentage of total conductivity (Campos et al., 2003).

2.3. Estimation of F^- bioaccumulation in rice tissues

0.2 g of shoot and root tissue was oven-dried, separately crushed in TISAB buffer and mineralized. The solution was centrifuged and the fluoride content in the clear extract was analyzed using a fluoride-sensitive electrode (Cole-Palmer, USA). Translocation factor (TF) was calculated as: fluoride content in shoot/fluoride content in root.

2.4. Analysis of parameters associated with oxidative damages: estimation of the contents of chlorophyll (Chl), malondialdehyde (MDA), hydrogen peroxide (H_2O_2) and protease activity

Chl was extracted from 0.4 g of freshly harvested tissue in 80% (v/v) chilled acetone. Total Chl, Chl a, and Chl b were measured according to Arnon (1949). The MDA content was calculated according to Roychoudhury et al. (2012) using 155 mM^{-1} cm^{-1} as the molar extinction coefficient of MDA. H_2O_2 content was spectrophotometrically measured at 390 nm and estimated from a standard curve (Velikova et al., 2000). The protease activity was measured using purified casein hydrolysate and enzyme extract following Roychoudhury et al. (2011).

2.5. Analysis of enzymes involved in Krebs cycle, sugar metabolism and nitrogen-assimilation: PyrDH (EC 1.2.4.1), MDH (EC 1.1.1.37), SDH (EC 1.3.5.1), α-amylase (EC 3.2.1.1) and NR (EC 1.7.99.4)

PyrDH activity was determined spectrophotometrically by measuring the formation of NADH at 340 nm. The experiment was performed following the protocol by Ke et al. (2014). For measuring MDH activity, 0.5 g freshly harvested tissue was ground in ice-cold crushing buffer containing 100 mM tricine, 1 mM EDTA, 5% (w/v) PVP, 20% (v/

Table 1
Physiological parameters and F^- bioaccumulation in the tissues of IR-64 and GB. The data are the mean values ($n = 3$) ± SE. SE ($p \leq 0.05$) is represented as '*' (for comparison within treatments) and as '#' (for comparison within cultivars). The symbols represent significance at $p \leq 0.05$.

Parameters	Analysis	IR-64 Control	IR-64 (15 mg L^{-1} NaF)	IR-64 (25 mg L^{-1} NaF)	GB Control	GB (15 mg L^{-1} NaF)	GB (25 mg L^{-1} NaF)
Physiological parameters	Percentage of germination	99 ± 1.0	93.5 ± 1.8	82.7 ± 2.1*	99 ± 0.5	97.2 ± 1.3	94.1 ± 2.5#
	Shoot length (cm)	13.2 ± 2.3	11.9 ± 1.5	9.7 ± 0.6*	7.2 ± 0.8#	7.1 ± 0.9#	7.0 ± 0.4#
	Root length (cm)	6.2 ± 0.7	3.1 ± 0.5*	2.7 ± 0.5	3.3 ± 0.2#	3.3 ± 0.7	3.4 ± 0.2
	Percentage of EL	14.2 ± 1.2	22.1 ± 1.7*	26.9 ± 2.3*	22.9 ± 1.8#	17.3 ± 2.3*#	17.4 ± 1.9#
F^- content	Shoot (mg g^{-1} FW)	0.7 ± 0.1	4.2 ± 0.5*	38.4 ± 8.1*	0.2 ± 0.1#	5.0 ± 0.8*#	8.1 ± 2.1*#
	Root (mg g^{-1} FW)	0.8 ± 0.1	2.7 ± 0.4*	47.6 ± 10.3*	0.3 ± 0.1#	5.9 ± 1.1*#	5.9 ± 1.4#

v) glycerol and 4 mM β-mercaptoethanol. The reaction mixture consisted of 0.1 (M) potassium phosphate buffer (pH 7.4), 0.00375 (M) NADH, 0.006 (M) oxaloacetic acid (freshly prepared) and crude enzyme extract. The MDH activity was determined by measuring the decrease in NADH at 340 nm and by using the extinction coefficient of 6.22 mM^{-1} cm^{-1}. The SDH activity was measured by documenting the formation of reduced 2-(p-iodophenyl)-3-(p-nitrophenyl)-5-phenyltetrazolium chloride [INT] or INT-formazan at 458 nm. The enzyme extract was prepared from 0.5 g tissue using the same crushing buffer used for measuring MDH activity. The molar extinction coefficient of 18000 M^{-1} cm^{-1} was used to calculate concentration of INT-formazan formed at 458 nm (Green and Narahara, 1980). The activity of α-amylase was measured according to Chrispeels and Varner (1967) after inactivating β-amylase by heating the extract at 70 °C for 5 min in presence of 9 mM $CaCl_2$. The NR activity was assayed according to Roychoudhury et al. (2016) by measuring the absorbance at 540 nm. The actual concentration of the enzyme was determined from a standard curve generated from increasing concentrations of potassium nitrite.

2.6. Expression analysis of genes

The seedlings (100 mg) from each of the experimental sets were used for RNA isolation. Total RNA was isolated using RNAisoplus (Takara, Japan) following the manufacturer's instructions. The concentration and purity of the isolated RNA was checked spectrophotometrically. The primers were designed using online NCBI Primer-blast (http://www.ncbi.nlm.gov/tools/primer-blast/index) software. Total RNA was treated with DNase I (Thermo Scientific) to remove DNA contamination. About 5 μg of total RNA was reverse-transcribed using Maxima First Strand cDNA synthesis kit (Thermo Scientific). Comparative RT-PCR analysis was performed using gene-specific primers and standard reagents, with *β-actin* as internal control as described earlier (Paul and Roychoudhury, 2018).

2.7. Immunoblot analysis of P-H^+/ATPase transporter

Total protein isolation from 1 g of control and salt-treated seedlings was performed according to Roychoudhury et al. (2008) and the concentration of the protein was estimated through Bradford analysis, which was replicated at least three times for each sample (Bradford, 1976). Based on such analysis, 100 μg of total protein was transferred onto nitrocellulose membrane (GE Healthcare, USA) using Mini Trans-Blot Cell (Bio-Rad, USA). This was followed by incubating the membrane in anti-P-H^+/ATPase primary antibody (a generous gift from Dr. Marc Boutry) at 1:4000 dilutions. The P-H^+/ATPase protein bands were detected by incubating the membrane in substrate solution containing nitroblue tetrazolium-5-bromo-4-chloro-3-indolyl phosphate (NBT-BCIP) (Sambrook and Russell, 2001).

2.8. Protein estimation

Total protein content was estimated according to Bradford (1976) using bovine serum albumin (BSA) as standard for all enzyme assays. In all the experiments, equal amounts of total protein from all the sample sets were used.

2.9. Statistical analysis

The statistical analyses were performed in completely randomized design (CRD) using three replicates (n = 3) with each replication containing an average of 50 seeds. The error bars in the graphs represent means ± standard error (SE). The statistical significance was calculated using two way analysis of variance (ANOVA) at $p \leq 0.05$. The calculations were performed using XLSTAT 2018.

3. Results

3.1. Analysis of the basic physiological parameters affected by fluoride stress

The percentage of germination of seedlings reduced in IR-64 seeds imbibed in 25 mg L^{-1} NaF compared to those in water (control) and 15 mg L^{-1} NaF (Table 1). The reduction in percentage of germination was comparatively less in GB exposed to fluoride stress, and was not statistically significant (Table 1). The shoot length (SL) was found to decrease in IR-64 with increasing fluoride concentration (Table 1). However, SL was not affected by F^- in case of GB seedlings even after 20 days. The drastic reduction in root length (RL) was observed in IR-64 exposed to F^- stress (Table 1). The RL decreased by about 2.3-fold in IR-64 grown in 25 mg L^{-1} NaF compared to that in the control seedlings. Interestingly, RL slightly increased in GB seedlings with increasing concentration of F^-.

The EL significantly increased in both F^--treated sets of IR-64 compared to control seedlings. The EL was about 1.9-fold higher in NaF (25 mg L^{-1})-stressed IR-64 compared to the control seedlings. However, the EL decreased in the stressed seedlings of GB compared to that in the control (Table 1).

3.2. Bioaccumulation of F^-

IR-64 accumulated 4.21 mg g^{-1} and 2.67 mg g^{-1} on an average in the shoots and roots respectively on exposure to 15 mg L^{-1} NaF stress. Application of 25 mg L^{-1} of NaF increased F^- bioaccumulation by about 9.1-fold in the shoots and almost 17.8-fold in the roots in IR-64 compared to the seedlings treated with 15 mg L^{-1} NaF (Table 1).

F^- bioaccumulation was higher in the shoots and roots of NaF (15 mg L^{-1})-stressed GB compared to the IR-64 counterpart. However, F^- accumulation did not increase significantly in GB seedlings exposed to 25 mg L^{-1} of F^- stress and was much less compared to the NaF (25 mg L^{-1})-stressed IR-64 seedlings (Table 1). Application of 15 mg L^{-1} of NaF increased F^- accumulation to 5.0 mg g^{-1} and

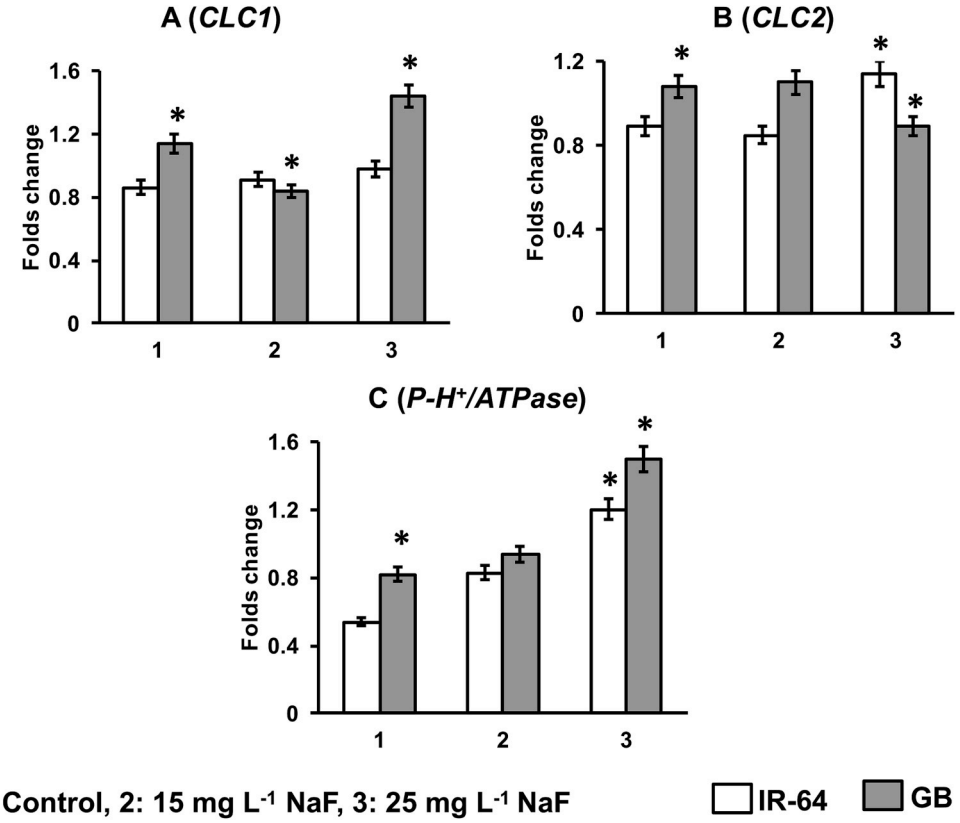

Fig. 1. Transcript level of *CLC1* (A), *CLC2* (B) and *P-H$^+$/ATPase* (C) in IR-64 and GB seedlings grown with double distilled water (control), 15 mg L^{-1} NaF and 25 mg L^{-1} NaF. The data are the mean values (n = 3) ± standard error (SE). The SE ($p \leq 0.05$) in each case is represented by the vertical bar in each graph. '*' designated on top of the bars represent significance at $p \leq 0.05$.

5.9 mg g^{-1} in the shoots and roots of GB respectively. Under higher stress exposure, GB seedlings accumulated 8.1 mg g^{-1} F^- on an average in the shoots. However, the average F^- content in the roots remained unchanged compared to that under 15 mg L^{-1} F^- stress. During 25 mg L^{-1} of F^- stress, GB exhibited a TF of 1.37.

3.3. Expression of membrane channels involved in F^- transport and proton homeostasis

CLC1 was marginally up regulated in IR-64 during increasing concentrations of F^-. However, it was significantly down regulated in GB during 15 mg L^{-1} of NaF stress and again markedly induced at 25 mg L^{-1} NaF stress (Fig. 1A). The higher F^- concentration significantly induced and down regulated *CLC2* expression in IR-64 and GB respectively. No significant alteration in the expression of this gene was observed for 15 mg L^{-1} NaF stress in both the varieties (Fig. 1B). Expression of *P-H$^+$/ATPase* was gradually increased in both the varieties under increasing concentrations of NaF. The expression of this gene was maintained at a higher level in GB compared to IR-64 under all the conditions (Fig. 1C).

3.4. Immunoblot against P-H$^+$/ATPase

Equal loading of protein samples has been represented by the total protein profile on 12% sodium dodecyl sulphate polyacrylamide gel (Fig. 2A). The immunoblot analyses revealed that in line with *P-H$^+$/ATPase* expression, increasing concentrations of NaF stimulated higher accumulation of P-H$^+$/ATPase in both the cultivars (Fig. 2B). The accumulation of P-H$^+$/ATPase under 25 mg L^{-1} of NaF stress in GB was much higher than that in IR-64 seedlings treated with the same concentration of NaF.

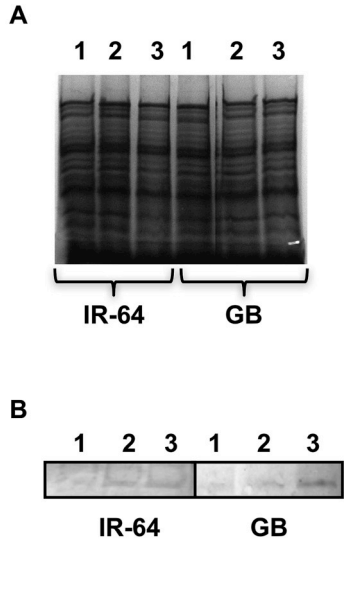

Fig. 2. SDS-PAGE representing loading of equal amount of total protein isolated from IR-64 and GB seedlings grown with double distilled water (control), 15 mg L^{-1} NaF and 25 mg L^{-1} NaF (A); protein immunoblot analysis with P-H$^+$/ATPase antibody showing higher accumulation of the transporter protein during increasing F^- concentrations in both the varieties (B).

3.5. Biochemical parameters associated with oxidative damages

Total chlorophyll (Chl), along with Chl a and Chl b contents were significantly reduced in IR-64 seedlings exposed to 15 mg L^{-1} and further decreased during 25 mg L^{-1} of F^- stress (Fig. 3A). The total Chl content decreased by about 1.6-fold in NaF (25 mg L^{-1})-stressed IR-64

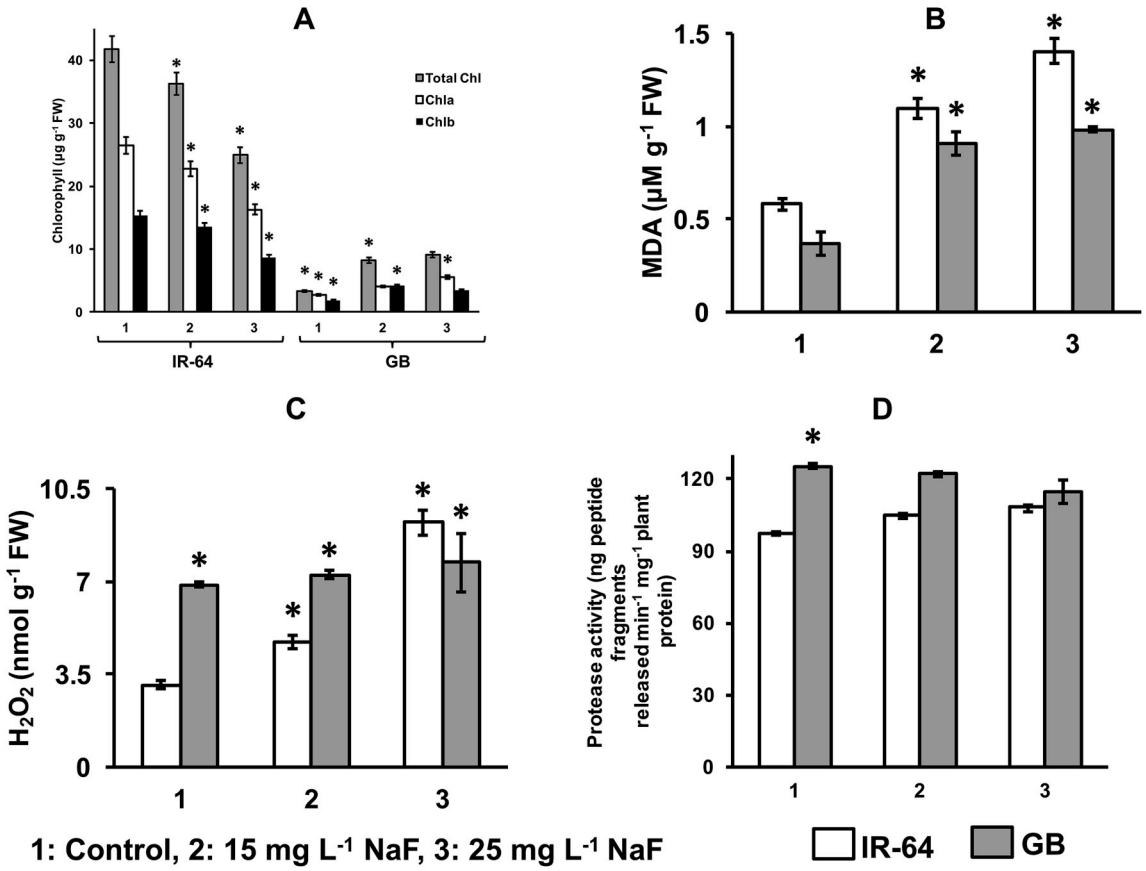

Fig. 3. Level of Chl (A), MDA (B), H_2O_2 (C) and activity of protease (D) in IR-64 and GB seedlings grown with double distilled water (control), 15 mg L^{-1} NaF and 25 mg L^{-1} NaF. The data are the mean values ($n = 3$) ± standard error (SE). The SE ($p \leq 0.05$) in each case is represented by the vertical bar in each graph. '*' designated on top of the bars represent significance at $p \leq 0.05$.

seedlings compared to that in the control. Total Chl, Chl a and Chl b contents increased in GB seedlings exposed to 15 mg L^{-1} stress as compared to the control set. Total Chl content remained unchanged in case of NaF (25 mg L^{-1})-stressed GB as compared to the NaF (15 mg L^{-1})-stressed seedlings. The Chl a content increased, whereas Chl b content decreased in NaF (25 mg L^{-1})-stressed GB as compared to the NaF (15 mg L^{-1})-stressed seedlings (Fig. 3A). The MDA content steeply increased in both IR-64 and GB seedlings under gradually increasing F^- stress. IR-64 accumulated higher MDA level under all the conditions as compared to GB (Fig. 3B). GB accumulated higher H_2O_2 level as compared to IR-64 during 15 mg L^{-1} stress. However, the H_2O_2 content increased drastically in IR-64 during 25 mg L^{-1} stress, showing even higher level than that in GB (Fig. 3C). Increasing fluoride concentrations slightly increased protease activity (not statistically significant) in IR-64. However the protease activity was gradually reduced in case of stressed GB seedlings compared to the control (Fig. 3D).

3.6. Activity of enzymes involved in Krebs cycle, sugar metabolism and nitrogen assimilation

The PyrDH activity decreased significantly in IR-64 seedlings exposed to 15 mg L^{-1} of NaF stress. The activity decreased by 1.4-fold during 25 mg L^{-1} stress compared to that in control seedlings. The enzyme activity was almost unaffected in GB exposed to both the concentrations of fluoride (Fig. 4A). F^- stress inhibited the SDH activity in IR-64 similar to PyrDH, whereas increasing F^- stress triggered SDH activity in GB (Fig. 4B). The MDH activity significantly increased in F^--stressed IR-64, as compared to control. However, the MDH activity in GB increased during 15 mg L^{-1} stress, but was decreased (reverting back to that in control) during 25 mg L^{-1} stress (Fig. 4C). The α-amylase activity decreased in F^--stressed IR-64 and increased in stressed GB compared to their respective control sets (Fig. 4D). The NR activity significantly decreased in IR-64 plants grown under 15 mg L^{-1} of NaF. However, the activity increased marginally during 25 mg L^{-1} stress. Similar trend was observed in case of GB, though the NR activity was maintained at a greater level in stressed GB compared to the stressed IR-64 seedlings (Fig. 4E).

3.7. Expression of genes involved in sugar metabolism, photosynthesis and glycolysis

The expression of *α-amylase* was almost similar in control and NaF-stressed IR-64 seedlings. The expression of *α-amylase* was likewise similar in control and 15 mg L^{-1} NaF-stressed GB seedlings, whereas the gene was strongly induced in GB during 25 mg L^{-1} F^- stress (Fig. 5A). The *RuBisCo* was gradually down regulated by F^- stress in both the cultivars. However, GB maintained higher *RuBisCo* expression compared to IR-64 under all the conditions (Fig. 5B). The expression of *phosphofructokinase* was triggered in both the cultivars in response to F^- stress. The gene was up regulated to a much higher extent in GB compared to IR-64 during stress (Fig. 5C). The *FBPase* expression slightly decreased in IR-64 during 15 mg L^{-1} NaF stress, but was significantly induced in IR-64 exposed to 25 mg L^{-1} of F^- stress. Exposure to 15 mg L^{-1} NaF stress down regulated *FBPase* expression in GB seedlings. A similar decreased transcript level for *FBPase* was also observed for GB exposed to 25 mg L^{-1} NaF (Fig. 5D). The *PGmutase* was down regulated in IR-64 and GB during 15 mg L^{-1} of F^- stress and was significantly induced during exposure to 25 mg L^{-1} of NaF. However, GB maintained higher transcript level of *PGmutase* compared to IR-64 under both the concentrations of F^- stress (Fig. 5E).

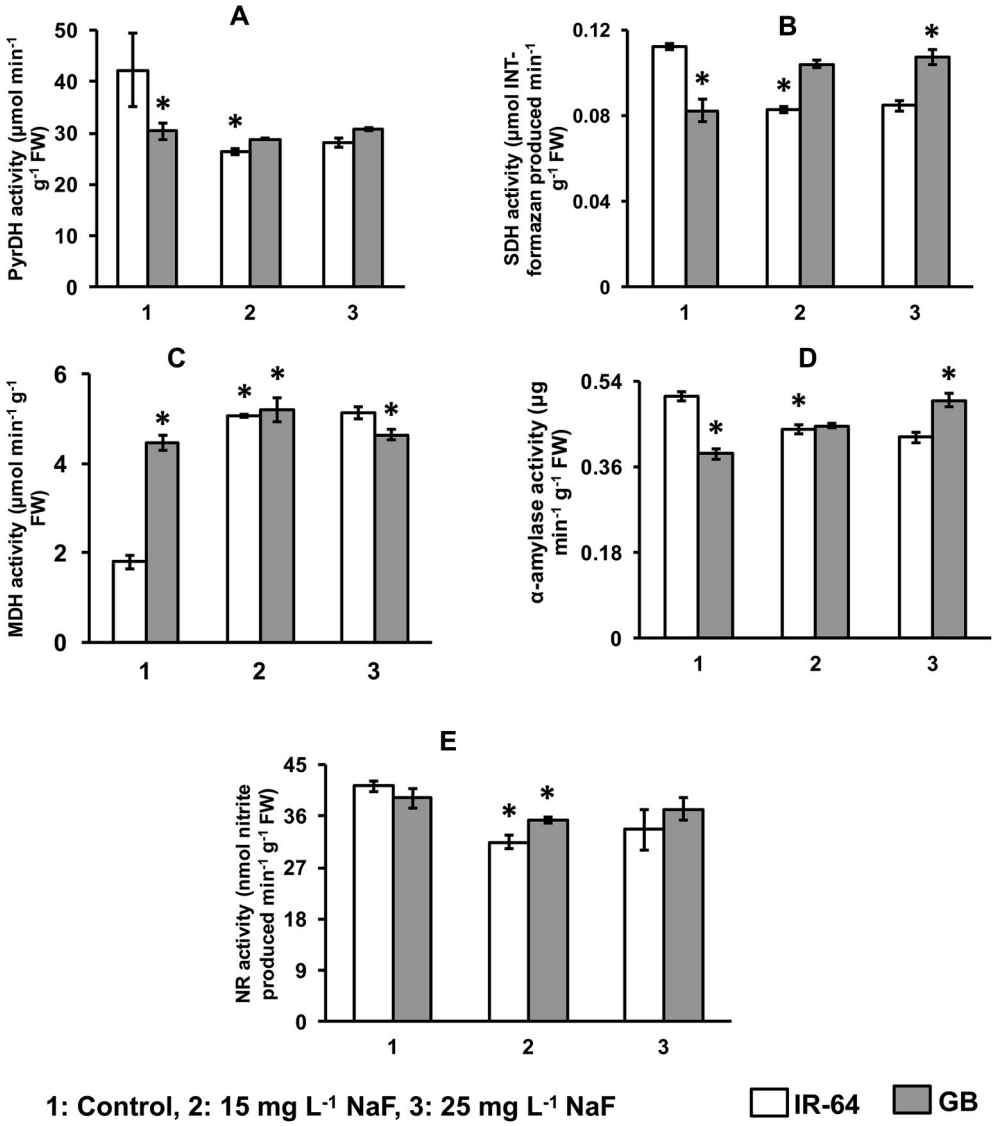

Fig. 4. Activity of enzymes like PyrDH (A), SDH (B), MDH (C), α-amylase (D) and NR (E) in IR-64 and GB seedlings grown with double distilled water (control), 15 mg L^{-1} NaF and 25 mg L^{-1} NaF. The data are the mean values ($n = 3$) ± standard error (SE). The SE ($p \leq 0.05$) in each case is represented by the vertical bar in each graph. '*' designated on top of the bars represent significance at $p \leq 0.05$.

4. Discussion

The detailed analysis of the physiological parameters indicated that unlike IR-64, GB was not drastically affected by increasing concentrations of F^- stress. Due to lower F^- uptake, GB accumulated lower endogenous F^- within the tissues. As a result, GB was able to maintain higher RL and low EL due to lesser extent of membrane damage. GB endured F^- stress by restricting its uptake, as a result of which excess F^- ions were not available for Chl degradation, which was pronounced in the case of fluoride-treated IR-64. This was also manifested by the slower rate of suppression of *RuBisCo* gene and lowered protease activity in GB. IR-64 exhibited high susceptibility to NaF stress based on the above parameters and also accumulated higher MDA and H_2O_2 compared to GB. It is known that any kind of oxidative stress negatively affects photosynthesis by degrading chlorophyll and reducing the *RuBisCo* transcript level (Roychoudhury et al., 2012; Parry et al., 2002; Mondal, 2017). The F^- bioaccumulation beyond 1.5 µg g^{-1} tissue could be detrimental for the grazing livestock (Banerjee and Roychoudhury, 2019). The extent of F^- accumulation in the roots and shoots of IR-64 and GB was several times higher than the prescribed safe limit, signifying a potential biohazard. Our observation also showed that beyond 15 mg L^{-1} NaF stress, IR-64 accumulated F^- in an uncontrollable manner, whereas F^- content in the NaF (25 mg L^{-1})-stressed GB seedlings was close to that during 15 mg L^{-1} NaF stress. This showed that GB was able to regulate the entry of excess F^- ions in a much organized manner as compared to IR-64. Two vacuolar voltage gated chloride channels (CLC1 and CLC2) have been identified in rice (Nakamura et al., 2006). The expression of *CLC1* and not *CLC2* was induced on exposure to NaCl (Nakamura et al., 2006). F^- ions are easily absorbed through roots via the chloride channels, which have larger passage diameter than F^- ions. The analysis of the transcript level of channel proteins showed that *CLC2* might be predominantly involved in F^- entry and hence the gene was significantly down regulated and up regulated in NaF (25 mg L^{-1})-stressed GB and IR-64 respectively. On the contrary, the expression pattern of *CLC1* indicated that it might not be the major regulator during entry of excess F^- ions. The P-H^+/ATPase is directly involved in maintaining the proton gradient across the cell which requires extensive maintenance during negatively charged ionic stress like F^-. Baunthiyal and Sharma (2014) reported reduced P-H^+/ATPase activity in the semi-arid F^- hyperaccumulator plants, *Acacia tortilis*, *Cassia fistula* and *Prosopis juliflora* exposed to fluoride stress. However, we observed that the transcript

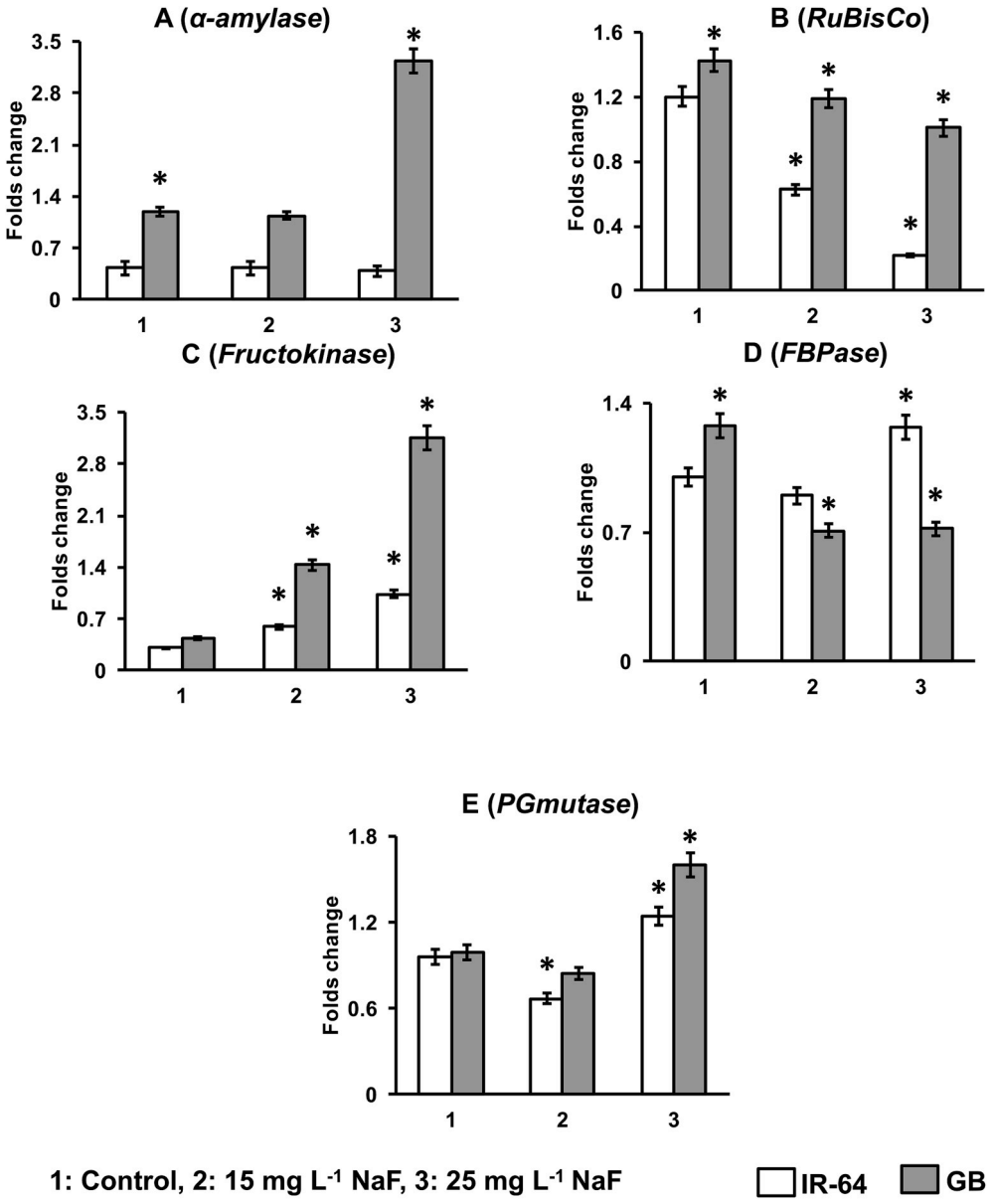

Fig. 5. Transcript level of *α-amylase* (A), *RuBisCo* (B), *fructokinase* (C), *FBPase* (D) and *PGmutase* (E) in IR-64 and GB seedlings grown with double distilled water (control), 15 mg L^{-1} NaF and 25 mg L^{-1} NaF. The data are the mean values ($n = 3$) ± standard error (SE). The SE ($p \leq 0.05$) in each case is represented by the vertical bar in each graph. '*' designated on top of the bars represent significance at $p \leq 0.05$.

and protein accumulation increased in the two rice varieties under both the concentrations of NaF stress. The NaF (25 mg L^{-1})-stressed-GB plants accumulated much higher level of P-H^+/ATPase as compared to IR-64 and hence could better maintain cellular homeostasis during stress.

Sugar metabolism during F^- stress exhibited another instance of varietal difference. The expression of *phosphofructokinase*, the rate limiting enzyme of glycolysis clearly highlighted that GB could modulate the overall pathway in a much more efficient fashion compared to IR-64. Upon monitoring the *FBPase* expression, it could be inferred that glycolysis is partially inhibited in IR-64 exposed to increasing concentrations of F^-. GB, on the other hand, showed down regulated expression of *FBPase* so as to efficiently operate the pathway during F^- stress. The expression pattern of *PGmutase* indicated inhibition in the conversion of glucose-1-phosphate to glucose-6-phosphate, the starting material for glycolysis in both the varieties during 15 mg L^{-1} of NaF stress. However, during 25 mg L^{-1} of NaF stress, the gene expression pattern indicated towards stimulated conversion of glucose-1-phosphate to glucose-6-phosphate in GB, as compared to IR-64, thereby highlighting again the efficient operation of glycolysis in GB during higher F^- stress. The glycolytic pathway seemed to be less operative during NaF-mediated stress in IR-64. F^- stress inhibited the Krebs cycle in IR-64 by suppressing the activity of the rate limiting enzyme, PyrDH and subsequently SDH. Increased MDH activity in stressed IR-64 indicated that the plant metabolism increased the oxaloacetate level, producing more substrate for the inhibited cycle. GB, on the contrary, increased the activity of the enzymes involved in Krebs cycle during F^- stress, establishing the well-adaptive behaviour. These enzymes are also reported to be strongly inhibited by high salt concentrations in C3 plants (Che-Othman et al., 2017). Higher α-amylase activity and transcript level in GB ensured more efficient sugar metabolism and growth responses during F^- stress. Based on the activity of NR, nitrogen assimilation appeared to be inhibited in both the cultivars upon exposure to high F^- stress.

Overall, F^- stress largely triggered membrane damage and inhibition of photosynthesis, sugar metabolism, glycolysis and Krebs cycle in

the susceptible cultivar IR-64. This variety exhibited bioaccumulation of F^- in toxic levels when exposed to 25 mg L^{-1} NaF. The aromatic cultivar, GB on the contrary accumulated much lower amounts of toxic F^- ions depicting the regulated entry of F^- and the phenotypic variations. CLC2 rather than CLC1 appeared to be involved in F^- uptake. Due to regulated F^- entry, the extent of damage was significantly less in GB compared to IR-64. The aromatic cultivar maintained photosynthesis, sugar metabolism, glycolysis and Krebs cycle even under high concentration of F^- stress. However, nitrogen assimilation was found to decline in both the varieties exposed to stress. The current study clearly illustrates the injurious effects of F^- on two differentially-responsive rice cultivars and also verifies the potential biohazard caused by the xenobiotic upon accumulation in rice tissues. The guiding significance of the major results of this work for safe rice agriculture is mainly to prohibit the use of groundwater containing high amounts of F^- for rice cultivation. In addition, the cultivation of IR-64 seedlings in areas infested with F^- contaminated groundwater and also in land stretches with high soil F^- content should be avoided in order to maintain the quality and safety of the entire food chain.

Author contribution statement

Mr. Aditya Banerjee performed all the experiments and drafted the manuscript. Dr. Aryadeep Roychoudhury designed all the experiments, supervised the overall work, critically reviewed the manuscript and incorporated necessary modifications. Ms. Puja Ghosh assisted during the RNA isolation process.

Acknowledgement

Financial assistance from Science and Engineering Research Board, Government of India through the grant [EMR/2016/004799] and Department of Higher Education, Science and Technology and Biotechnology, Government of West Bengal, through the grant [264(Sanc.)/ST/P/S&T/1G-80/2017] to Dr. Aryadeep Roychoudhury is gratefully acknowledged. The authors thank Dr. Marc Boutry, Unité de Biochimie Physiologique, Université Catholique de Louvain, Belgium, for providing the anti-P-H^+/ATPase primary antibody as a kind gift. Mr. Aditya Banerjee is thankful to University Grants Commission, Government of India for providing Junior Research Fellowship in course of this work.

References

Arnon, D.I., 1949. Copper enzymes in isolated chloroplasts polyphenol oxidase in *Beta vulgaris*. Plant Physiol. 24, 1–15.

Banerjee, A., Roychoudhury, A., 2019. Differential regulation of defence pathways in aromatic and non-aromatic indica rice cultivars towards fluoride toxicity. Plant Cell Rep. https://doi.org/10.1007/s00299-019-02438-6.

Banerjee, A., Roychoudhury, A., 2019a. Fluorine: a biohazardous agent for plants and phytoremediation strategies for its removal from the environment. Biol. Plant. 63, 104–112.

Banerjee, A., Roychoudhury, A., 2019b. Structural introspection of a putative fluoride transporter in plants. 3 Biotech 9, 103.

Baunthiyal, M., Sharma, V., 2014. Response of fluoride stress on plasma membrane H^+-ATPase and vacuolar H^+-ATPase activity in semi-arid plants. Indian J. Plant Physiol. 19, 210–214.

Bradford, M.M., 1976. A rapid and sensitive method for the quantitation of microgram quantities of protein utilizing the principle of protein-dye binding. Anal. Biochem. 72, 248–254.

Campos, P.S., Quartin, V., Ramalho, J.C., Nunes, M.A., 2003. Electrolyte leakage and lipid degradation account for cold sensitivity in leaves of *Coffea* sp. plants. J. Plant Physiol. 160, 283–292.

Che-Othman, M.H., Millar, A.H., Taylor, N.L., 2017. Connecting salt stress signalling pathways with salinity-induced changes in mitochondrial metabolic processes in C3 plants. Plant Cell Environ. 40, 2875–2905.

Choubisa, S.L., 2013. Fluoride toxicosis in immature herbivorous domestic animals living in low fluoride water endemic areas of Rajasthan, India: an observational survey. Fluoride 46, 19–24.

Chrispeels, M.J., Varner, J.E., 1967. Gibberellic acid-enhanced synthesis and release of α-amylase and ribonuclease by isolated barley and aleurone layers. Plant Physiol. 42, 398–406.

Debska, K., Bogatek, R., Gniazdowska, A., 2012. Protein carbonylation and its role in physiological processes in plants. Postepy Biochem. 58, 34–43.

Green, J.D., Narahara, H.T., 1980. Assay of succinate dehydrogenase activity by the tetrazolium method: evaluation of an improved technique in skeletal muscle fractions. J. Histochem. Cytochem. 28, 408–412.

Gupta, S., Banerjee, S., Mondal, S., 2009. Phytotoxicity of fluoride in the germination of paddy (*Oryza sativa*) and its effect on the physiology and biochemistry of germinated seedlings. Fluoride 42, 142–146.

Ke, C.-J., He, Y.-H., He, H.-W., Yang, X., Li, R., Yuan, J., 2014. A new spectrophotometric assay for measuring pyruvate dehydrogenase complex activity: a comparative evaluation. Analyt. Methods 6, 6381–6388.

Mackill, D.J., Khush, G.S., 2018. IR64: a high-quality and high-yielding mega variety. Rice 11, 18.

Meenakshi, R.C. Maheshwari, 2006. Fluoride in drinking water and its removal. J. Hazard Mater. 137, 456–463.

Mondal, N.K., 2017. Effect of fluoride on photosynthesis, growth and accumulation of four widely cultivated rice (*Oryza sativa* L.) varieties in India, Ecotoxicol. Environ. Saf. 144, 36–44.

Mondal, D., Gupta, S., 2015. Influence of fluoride contaminated irrigation water on biochemical constituents of different crops and vegetables with an implication to human risk through diet. J. Mater. Environ. Sci. 6 3134-3132.

Nakamura, A., Fukuda, A., Sakai, S., Tanaka, Y., 2006. Molecular cloning, functional expression and subcellular localization of two putative vacuolar voltage-gated chloride channels in rice (*Oryza sativa* L.). Plant Cell Physiol. 47, 32–42.

Parry, M.A.J., Andralojc, P.J., Khan, S., Lea, P.J., Keys, A.J., 2002. Rubisco activity: effects of drought stress. Ann. Bot. 89, 833–839.

Paul, S., Roychoudhury, A., 2018. Transcriptome profiling of abiotic stress-responsive genes during cadmium chloride-mediated stress in two indica rice varieties. J. Plant Growth Regul. 37, 657–667.

Rao, B.V.A., Kumar, A.K., Nagalaksmamma, K., Vidyunmala, S., 2013. Effect of fluoride on protein profiles in two cultivars of mulberry leaves. AE J. Agric. Environ. Sci. 13, 957–960.

Roychoudhury, A., Basu, S., Sarkar, S.N., Sengupta, D.N., 2008. Comparative physiological and molecular responses of a common aromatic indica rice cultivar to high salinity with non-aromatic indica rice cultivars. Plant Cell Rep. 27, 1395–1410.

Roychoudhury, A., Basu, S., Sengupta, D.N., 2011. Amelioration of salinity stress by exogenously applied spermidine or spermine in three varieties of indica rice differing in their level of salt tolerance. J. Plant Physiol. 168, 317–328.

Roychoudhury, A., Basu, S., Sengupta, D.N., 2012. Antioxidants and stress-related metabolites in the seedlings of two indica rice varieties exposed to cadmium chloride toxicity. Acta Physiol. Plant. 34, 835–847.

Roychoudhury, A., Ghosh, S., Paul, S., Mazumdar, S., Das, G., Das, G., 2016. Pre-treatment of seeds with salicylic acid attenuates cadmium chloride-induced oxidative damages in the seedlings of mungbean (*Vigna radiata* L. Wilczek). Acta Physiol. Plant. 38, 11.

Sambrook, J., Russell, D.W., 2001. Molecular Cloning : a Laboratory Manual. Cold Spring Harbor Laboratory Press, New York, pp. 114–115.

Susheela, A.K., 1999. Fluorosis management programme in India. Curr. Sci. 77, 10.

Velikova, V., Yordanov, I., Edreva, A., 2000. Oxidative stress and some antioxidant systems in acid rain treated bean plants. Protective role of exogenous polyamines. Plant Sci. 151, 59–66.